Small-Angle X-Ray and Light Scattering Studies on the Influence of Mg^{2+} Ions on the Structure of the RNA from Bacteriophage MS2

Gertraud Ribitsch [a], Rita De Clercq [b], Waltraud Folkhard [a,*], Peter Zipper [a], Josef Schurz [a], and Julius Clauwaert [c]

[a] Institut für Physikalische Chemie, Universität Graz, Heinrichstr. 28, A-8010 Graz, Austria
[b] Laboratorium voor Fysiologische Chemie, Rijksuniversiteit Gent, B-9000 Gent, Belgium
[c] Departement Biochemie, Universitaire Instelling Antwerpen, B-2610 Wilrijk, Belgium

Z. Naturforsch. **40 c**, 234–241 (1985); received August 20/December 14, 1984

RNA, Interaction with Mg^{2+}, Small-Angle X-Ray Scattering, Light Scattering, Structural Changes

The influence of Mg^{2+} ions on the secondary and tertiary structure of the RNA from bacteriophage MS2 was investigated by small-angle X-ray scattering and light scattering and by sedimentation experiments.

The analysis of the outer part of the X-ray scattering curve obtained at low temperature in the absence of Mg^{2+} yielded a cross-section radius of gyration of 0.88 nm and a mass per unit length of 1720 g mol^{-1} nm^{-1}. Very similar values for these parameters, which refer to the secondary structure of the RNA molecule, were also derived from the X-ray scattering curves obtained in the presence of different amounts of Mg^{2+} (0.07 to 1 ions per nucleotide). On the contrary, the inner part of the X-ray scattering curves turned out to be highly dependent on the Mg^{2+} concentration: the cross-section radius of gyration and the mass per unit length, which were determined from the scattering curves at small angles as parameters related to the tertiary structure of the RNA, amounted to 3.11 nm and 4000 g mol^{-1} nm^{-1}, respectively, in the absence of Mg^{2+} and increased significantly upon raising the concentration of Mg^{2+}. The increase of these structural parameters was found to be accompanied by a decrease of the overall radius of gyration (as revealed indirectly by X-ray scattering and directly by light scattering measurements) and by an increase of the sedimentation coefficient.

The results from the investigations of the RNA at low temperature clearly establish the existence of double-stranded structures down to very low Mg^{2+} concentrations as well as the occurrence of Mg^{2+} induced changes of the tertiary structure. In the absence of Mg^{2+} the RNA molecule appears to be a rodlike particle of about 300 nm length with a lateral diameter of about 9 to 11 nm. Upon addition of increasing amounts of Mg^{2+} this extended structure tightens, eventually forming a coil-like particle. Previous X-ray scattering experiments with MS2 RNA at ionic strength 0.1 (Zipper, Folkhard and Clauwaert, FEBS Lett. **56**, 283–287 (1975)) have already established the axial dimensions of such coil-like particles to be about 63, 31 and 14 nm.

The results from supplementary X-ray scattering experiments performed at higher temperatures in the absence or presence of Mg^{2+} clearly reflect the loss of secondary structure due to melting of the RNA. This loss is, however, less pronounced at higher concentrations of Mg^{2+}.

Introduction

As a consequence of the polyelectrolyte character of polynucleotides their conformation is strongly dependent on the concentration and nature of cations. In this way cations also strongly influence interactions between proteins and nucleic acids (*cf. e.g.* [1–6]). The fact that Mg^{2+} ions are integral components of biologically active RNAs such as tRNA, ribosomal RNA and viral RNA, and that they influence the structure and function of these RNAs has stimulated numerous studies on the interaction between Mg^{2+} and RNA.

While for tRNA the mode of binding, the number and location of binding sites, and the influence of this binding on the secondary and tertiary structure have been cleared up [7–13], the picture is less clear for the larger RNAs such as rRNA and viral RNA. From hydrodynamic studies it has been made clear that the presence of Mg^{2+} induces a tightening of rRNA [14–18]. Tight tertiary structures have also been suggested by small-angle X-ray scattering studies for the MS2 viral RNA at ionic strength 0.1 [19] and for 16 s rRNA [20]; based on the X-ray scattering curves, molecular models for these larger RNAs have been proposed.

* Present address: Pathologisches Institut der Universität Heidelberg, Abteilung für Ultrastrukturforschung, D-6900 Heidelberg, Bundesrepublik Deutschland

Reprint requests to Doz. Dr. Peter Zipper.

0341-0382/85/0300-0234 $ 01.30/0

As a continuation of our previous X-ray studies on large RNAs and in order to get further insight into the structural consequences of the interaction of Mg^{2+} with these RNAs, we studied in some detail the interaction of Mg^{2+} with MS2 viral RNA by applying small-angle X-ray scattering, light scattering and analytical boundary sedimentation. While these methods are generally known to be sensitive to the tertiary structure of biopolymers, in the case of nucleic acids the small-angle X-ray technique is additionally capable of yielding valuable informations on their secondary structure too (*cf.* [19–22]).

Materials and Methods

Preparation of the RNA solutions

The growth and purification of bacteriophage MS2 and subsequent isolation of viral RNA have been described previously [23]. Special attention has been paid to the careful sterilization of all glassware and solvents in order to avoid degradation of the RNA by ribonucleases as much as possible. To obtain Mg^{2+}-free RNA solutions, sufficient quantities of N-hydroxyethylethylendiamine triacetate were added to the isolation solvents in order to remove all Mg^{2+} ions. Stock solutions of RNA were prepared by dialysis against the desired buffer (0.2 mM Tris buffer pH 7.5; 0.2 mM Tris buffer pH 7.5, containing 10 mM NaCl; 10 mM Tris buffer pH 7.5; 2 mM phosphate buffer pH 6.4, containing 1 mM NaCl). Mg^{2+} ions were added to Mg^{2+}-free RNA solutions as $MgCl_2$ from carefully prepared and controlled stock solutions.

Small-angle X-ray scattering

Small-angle X-ray scattering (SAXS) experiments were performed by means of Kratky cameras [24, 25] and X-ray tubes with copper target ($\lambda = 0.154$ nm for Cu K_α line). If not stated otherwise, samples were investigated at 4 °C. The scattered radiation was detected by means of a proportional counter tube in the angular range $0.85 \leqq 2\theta \leqq 130$ mrad (corresponding to $0.035 \leqq h \leqq 5.3\ \mathrm{nm}^{-1}$, with $h = 4\pi \sin\theta/\lambda$). The intensity of the primary beam and the fraction of Cu K_β radiation were determined by using a Lupolen platelet [26, 27]. A set of computer programs [28–30] was used for the evaluation of the experimental data and for the elimination of collimation and wavelength effects. The interpretation of data was based on the well-known theory of SAXS [31]. Molecular masses were calculated by using the values for the isopotential specific volume v_2' that were derived from the densities of dialyzed RNA solutions and the dialysis buffers as measured at 4 °C by means of a digital density meter [32]. However, a rigorous application of multicomponent formalism [21, 33] was usually not possible since RNA solutions could not be dialyzed after the addition of defined amounts of Mg^{2+}.

Light scattering

Light scattering measurements were performed at 20 °C using a Sofica 42 000 light scattering photometer with non-polarized green light ($\lambda = 546$ nm). The light scattering was measured in an angular range from 45° to 135° for RNA concentrations between 80 and 200 µg/ml. Special attention has been paid to the removal of dust particles from the solvent and the solutions under ribonuclease-free conditions. Zimm plots were used to extrapolate the experimental data to zero angle and zero concentration, and to determine the radius of gyration R_G and the molar mass M. The R_G-values turned out to be almost independent of concentration. The M-values enabled a convenient control of the quality and homogeneity of the RNA samples as a value of 1.2×10^6 g mol^{-1} has to be expected for MS2 RNA.

Analytical boundary sedimentation

The sedimentation coefficients were measured in a Beckman Spinco model E analytical ultracentrifuge equipped with a photoelectron scanner and monochromator. All measurements were performed at 25 °C and rotor speed between 40 000 and 45 000 rpm with RNA solutions of concentrations between 10 and 50 µg/ml. The sedimentation coefficients were corrected for the primary charge effect by using the relation (*cf.* [34, 35])

$$\frac{s_{\text{observed}}}{s_{\text{corrected}}} = \frac{\chi_{\text{solvent}}}{\chi_{\text{solution}}} \quad (\chi : \text{conductivity}),$$

extrapolated to zero concentration, and reduced to standard conditions of 20 °C and water, yielding $s^0_{20,w}$.

Results

Hydrodynamic behaviour

Figure 1a shows the sedimentation coefficient $s^0_{20,w}$ as a function of the Mg^{2+}/phosphate ratio, for three different solvent conditions. There is a clear influence of the solvent composition at Mg^{2+}/phosphate ratios below 0.25, whereas at higher ratios the influence of solvent composition is much less pronounced. The increase of $s^0_{20,w}$ with increasing Mg^{2+}/phosphate ratio suggests that the RNA molecules tighten in the presence of Mg^{2+}. Similarly, the generally higher values for $s^0_{20,w}$ in the presence of 10 mM NaCl suggest that in this solvent the RNA molecules have a slightly more compact structure than in the absence of NaCl.

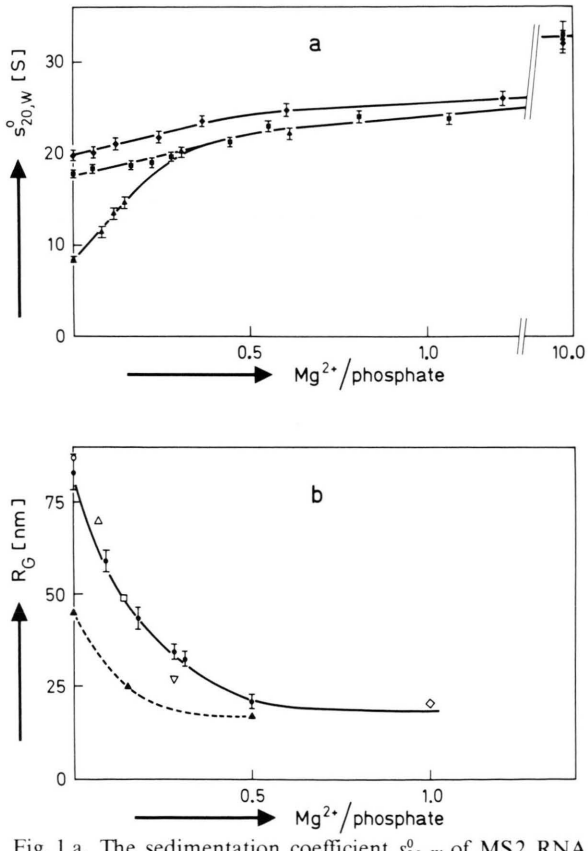

Fig. 1 a. The sedimentation coefficient $s^0_{20,w}$ of MS2 RNA at different Mg^{2+}/phosphate ratios and ionic strengths. ▲: 0.2 mM Tris buffer; ■: 10 mM Tris buffer; ◆: 0.2 mM Tris buffer containing 10 mM NaCl. b. Radius of gyration R_G of MS2 RNA in 0.2 mM Tris buffer at different Mg^{2+}/phosphate ratios. ●: experimental results from light scattering; ○, △, □, ▽, ◇: experimental results from X-ray scattering; ▲: values calculated from the experimental sedimentation coefficients by assuming spherical particles.

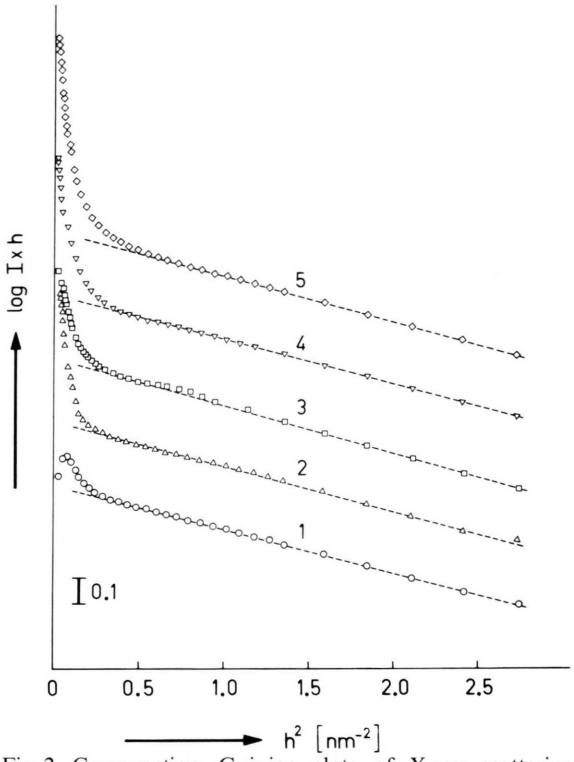

Fig. 2. Cross-section Guinier plots of X-ray scattering curves of MS2 RNA in 0.2 mM Tris buffer at 4 °C and different Mg^{2+}/phosphate ratios: *1* 0, *2* 0.07, *3* 0.14, *4* 0.28, *5* 1.0. The vertical position of the curves is arbitrary.

Light scattering

The experimental values obtained for the radius of gyration R_G of MS2 RNA in 0.2 mM Tris buffer are plotted in Fig. 1b *versus* the Mg^{2+}/phosphate ratio (solid curve). As can be seen, the radius of gyration drastically decreases upon raising the concentration of Mg^{2+}. This finding is qualitatively in agreement with the observed increase of $s^0_{20,w}$ under the same conditions. However there is a clear discrepancy between the experimental radii of gyration and the radii of gyration of the hydrodynamically equivalent spheres (dashed curve), which can be calculated from $s^0_{20,w}$ by using the relation

$$R_G = \frac{(3/5)^{1/2}\, M (1 - v'_2\, d)}{6\, \pi\, N\, \eta\, s^0_{20,w}}$$

This discrepancy suggests that the RNA molecules are of highly anisometric shape, particularly at low Mg^{2+} concentration.

Small-angle X-ray scattering

The Mg^{2+}-free RNA

The scattering curve obtained for Mg^{2+}-free RNA in 0.2 mM Tris buffer at a concentration of about 21 mg/ml is shown in a cross-section Guinier plot in Fig. 2 (curve 1). The curve is approximately linear over a wide angular range (for $h > 0.5$ nm^{-1}). This behaviour is indicative of rodlike structures. The slope of the straight line fitted to the curve in this angular range corresponds to a cross-section radius of gyration of 0.88 nm (cited in Table I as R_{c2}). The intercept of the straight line on the ordinate yields a mass per unit length of 1820 g mol^{-1} nm^{-1} (cited in Table I as M_{c2}); this value has been obtained by using the isopotential specific volume of $\bar{v}'_2$ = 0.482 ml/g as determined from another sample of Mg^{2+}-free RNA (see below).

As can further be seen from curve 1 of Fig. 2, the intensity increases towards the smallest angles in such a way that it rises above the straight line drawn through the outer part of the curve. The inner portion of the curve can also be approximated by a straight line fairly well; the slope and intercept of this line yield a second set of values for the cross-section radius of gyration and for the mass per unit length ($R_{c1} = 1.95$ nm, $M_{c1} = 2660$ g mol^{-1} nm^{-1}; *cf.* Table I).

Similar plots were also obtained for the scattering curves measured at lower concentrations of RNA. The results derived from these plots are also summarized in Table I. In order to eliminate the obvious influence of RNA concentration on the parameters R_{c1} and M_{c1}, these parameters were additionally extrapolated to zero concentration.

While the cross-section factor at larger angles, from which R_{c2} and M_{c2} were determined, is undoubtedly related to the secondary structure of the

Table I. Molecular parameters of MS2 RNA in 0.2 mM Tris buffer in the absence or presence of Mg^{2+}.

Mg^{2+} added (ions/nucleotide)	c [mg/ml]	R_{c1} [nm]	M_{c1} [g mol^{-1} nm^{-1}]	R_{c2} [nm]	M_{c2} [g mol^{-1} nm^{-1}]	L [nm]	R_G [nm]	
							SAXS	LS
0	21.1	1.95	2 660	0.88	1 820			
	16.9	2.35	2 930	0.88	1 750			
	10.6	2.52		0.88	1 720			
	0	3.11	4 000			300[a]	87[b]	83[c]
0.07	21.8			0.92	1 900			
	10.9	4.3	4 960	0.89	1 820	242[a]	70[b]	63[d]
0.09	0							59[c]
0.14	21.8	3.69	5 480	0.87	1 870			
	16.3	3.67	5 450					
	10.9	4.28	6 350	0.91	1 730			
	0	4.76	7 060			170[a]	49[b]	49[d]
0.18	0							43.5[c]
0.28	21.8	7.0	10 700	0.87	1 730			
	16.3	6.81						
	10.9	7.71	12 000	0.88	1 700			
	0	8.23	13 300			90[a]	27[b]	34.5[c]
0.31	0							32.5[c]
0.5	0							21[c]
1.0	7.2	8.47		0.89	1 590			
	0	8.47	33 100			69[e]	21.5[f]	

[a] Calculated from the ratio M/M_{c1} by assuming $M = 1.2 \times 10^6$ g mol^{-1}.
[b] Calculated from L and R_{c1}
[c] Directly determined by light scattering (c: 80 – 200 µg/ml); $M = (1.2 \pm 0.1) \times 10^6$ g mol^{-1}.
[d] Estimated from the solid curve in Fig. 4b.
[e] Determined from R_G and R_{c1}.
[f] Directly determined by SAXS (c: 2.4 – 7.2 mg/ml); $M = 2.5 \times 10^6$ g mol^{-1}.

RNA, the cross-section factor found at the small angles obviously reflects a higher-order structure. Possibly this cross-section factor is due to the overall shape of the RNA particle.

As the existence of a higher-order structure even in the absence of Mg^{2+} might be due to the possible presence of other cations, we tried to remove such ions by extensive dialysis of another sample of Mg^{2+}-free RNA against 0.2 mM Tris buffer. This extensively dialyzed sample was then also used for the determination of t'_2 as well as for SAXS experiments at higher temperatures (see below). A cross-section Guinier plot of the scattering curve of this sample at 4 °C is shown in Fig. 3a. This curve lacks the pronounced increase of intensity towards the smallest angles. The evaluation of the curve at larger angles ($h > 0.5\ nm^{-1}$) yields a cross-section radius of gyration $R_c = 0.97$ nm and a mass per unit length $M_c = 1510\ g\ mol^{-1}\ nm^{-1}$ (*cf.* Table II).

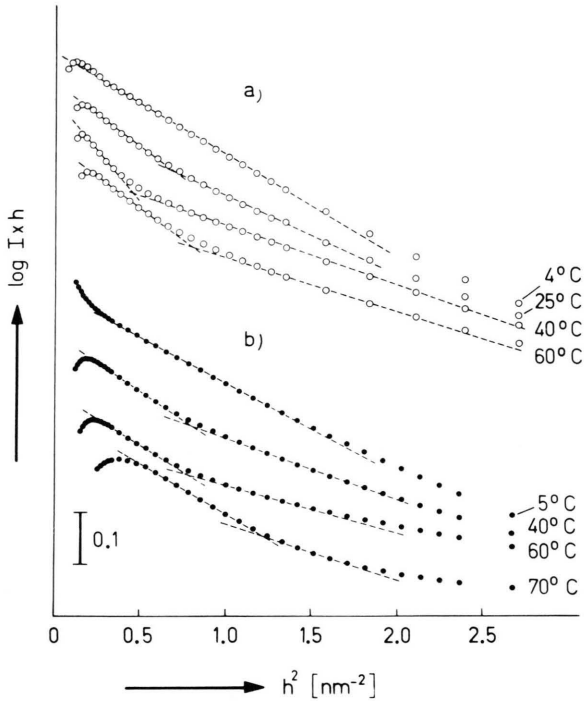

Fig. 3. Cross-section Guinier plots of X-ray scattering curves of MS2 RNA in 0.2 mM Tris buffer (a) and 2 mM phosphate buffer (b) at various temperatures. The vertical position of the curves is arbitrary.

The RNA at medium Mg^{2+} concentrations

The scattering curves obtained from measurements of the RNA in 0.2 mM Tris buffer at Mg^{2+}/phosphate ratios of 0.07, 0.14 and 0.28 were found to be similar to the curves for the Mg^{2+}-free RNA and were evaluated in an analogous way. The results are summarized in Table I; cross-section Guinier plots of the curves for the highest RNA concentrations are shown in Fig. 2 (curves 2–4).

As can be seen from Fig. 2 and Table I, significant changes in the scattering behaviour of the RNA upon addition of Mg^{2+} occur only in the innermost portion of the curves. These changes obviously reflect an increase of the cross-section radius of gyration R_{c1} and of the corresponding mass per unit length M_{c1} with increasing Mg^{2+} concentration. On the contrary, the scattering behaviour of the RNA at large angles ($h > 0.6\ nm^{-1}$) is not affected by the presence of Mg^{2+} ions to a significant extent. Particularly the values for R_{c2} are almost the same as for Mg^{2+}-free RNA.

Table II. Molecular parameters of MS2 RNA in different solvents at various temperatures.

Solvent	c [mg/ml]	t [°C]	R_c, R_{c1} [nm]	M_c, M_{c1} [g mol^{-1} nm^{-1}]	R_{c2} [nm]	M_{c2} [g mol^{-1} nm^{-1}]
Tris buffer, 0.2 mM	7.9	4	0.97	1 510		
		25	1.08	1 350	0.85	1 150
		40	1.37	960	0.74	710
		60	1.08	1 070	0.70	815
phosphate buffer, 2 mM	7.3	5	0.91	1 670		
		40	1.02	1 340	0.75	1 100
		60	0.98	870	0.66	710
		70	0.96	1 060	0.71	820

Estimation of particle size

The overall radius of gyration R_G of the RNA in the absence of Mg^{2+} or at medium Mg^{2+} concentrations could not be determined by means of SAXS in a direct way because the corresponding portion of the scattering curve was at unaccessibly small angles. However, an indirect estimation of R_G was attempted in the following way.

Due to the cross-section factor found at small scattering angles the RNA particle may be assumed to be elongate. In this case, the ratio of the molar mass M (assumed to be 1.2×10^6 g mol^{-1}) and the experimentally determined mass per unit length M_{c1} should yield an estimate for the length L of the particle. By combining L with the cross-section radius of gyration R_{c1}, an estimate for R_G may be obtained according to the relation $R_G^2 = R_{c1}^2 + L^2/12$. The values for L and R_G thus calculated are listed in Table I. As can be seen from the table and also from Fig. 1 b, the estimates for R_G agree fairly well with the radii of gyration that were determined directly by light scattering measurements.

The RNA at high Mg^{2+} concentration

A cross-section Guinier plot of the scattering curve of one sample of RNA to which 1 Mg^{2+} ion per nucleotide had been added is shown in Fig. 2 (curve 5). The course of the curve at larger angles corresponds to values of R_{c2} and M_{c2} which are very similar to those found at lower Mg^{2+} concentrations (*cf.* Table I). Unfortunately, this sample later on turned out to contain aggregates, probably dimers, instead of monomeric RNA molecules. Therefore neither the parameters R_{c1} and M_{c1} obtained for this sample nor the parameters L and R_G, which could in this case be determined directly from the scattering curve, can be regarded to be representative for the tertiary structure of RNA at high Mg^{2+} concentration. Nevertheless, the values for R_G and R_{c1} (*cf.* Table I) are similar to the corresponding parameters for "native" MS2 RNA as obtained previously [19].

Structural transitions induced by temperature

Cross-section Guinier plots of scattering curves obtained for Mg^{2+}-free RNA (dialyzed extensively against 0.2 mM Tris buffer) at various temperatures are shown in Fig. 3 a. These plots clearly reflect the occurrence of structural transitions at elevated temperatures. When the curves are approximated by straight lines as indicated in the figure, two sets of values are obtained for the cross-section radius of gyration and for the mass per unit length (*cf.* Table II). The drastic changes of the mass per unit length undoubtedly reflect a loss of secondary structure.

Similar scattering curves and results as for Mg^{2+}-free RNA in 0.2 mM Tris buffer were also obtained for RNA in 2 mM phosphate buffer (*cf.* Fig. 3 b and Table II). The mass per unit length was calculated in this case by using the value $v_2' = 0.457$ ml/g as determined previously [19].

Measurements of RNA in 0.2 mM Tris buffer at elevated temperatures in the presence of Mg^{2+} (0.14 and 0.28 Mg^{2+} ions added per nucleotide) did not show significant changes of the secondary-structure cross-section parameters at 40 °C or, for the higher Mg^{2+} concentration, even at 60 °C. At the same temperatures, however, the cross-section parameters related to the overall shape were significantly smaller than the corresponding values obtained at low temperature.

Discussion and Conclusions

The investigation of MS2 RNA in the presence of different amounts of Mg^{2+} and by different methods has yielded ample informations about the influence of Mg^{2+} ions on a variety of structural parameters. While most of these parameters (*viz.* $s^0_{20,w}$, R_G, R_{c1}, M_{c1}) are related to the tertiary structure of the RNA, the X-ray parameters R_{c2} and M_{c2} are sensitive to the secondary structure.

According to our results, the secondary structure of the RNA is unlikely to undergo drastic changes upon increasing the Mg^{2+} concentration. This conclusion is suggested by the lack of any systematic variation of R_{c2} and M_{c2} with the concentration of Mg^{2+} and by the fact that all values for R_{c2} and M_{c2} are close to the values of $R_{c2} = 0.91$ nm and $M_{c2} = 1690$ g mol^{-1} nm^{-1} obtained in the previous SAXS study of "native" MS2 RNA at ionic strength 0.1 (*cf.* [19]). The latter value of M_{c2} has been found to be consistent with a double-helix content of about 70% [36, 37]. Thus we may conclude that also at low Mg^{2+} concentrations and even in the absence of Mg^{2+} the fraction of nucleotides which are incor-

porated in double-helical structural elements is of similar magnitude as in the "native" RNA. The existence of double-helical structures even in the absence of Mg^{2+} has also been suggested by the results from UV and IR spectroscopy [35].

On the contrary, the tertiary structure of MS2 RNA appears to be highly dependent on the Mg^{2+} content: All results indicate a structural transition from an extended form in the absence of Mg^{2+} to a more compact form in the presence of Mg^{2+}. An inspection of the various structural parameters (*cf.* Fig. 1 and Table I) reveals that their most pronounced changes occur at Mg^{2+}/phosphate ratios below 0.28, whereas the additional changes occurring up to high Mg^{2+}/phosphate ratios or high ionic strength are comparably small (it should be noted that the value obtained for M_{cl} at a Mg^{2+}/phosphate ratio of 1.0 is not relevant in this context because it refers to a dimer; the corresponding parameter for the "native" RNA is $M_{cl} = 18\,900$ g mol^{-1} nm^{-1} [19]). This behaviour is again in good accord with the results from UV absorption [35] which reflected significant increases in base-pairing at Mg^{2+}/phosphate ratios below 0.25 and only smaller additional increases at higher Mg^{2+} concentrations.

A detailed analysis of the tertiary-structure cross-section parameters in connection with our previous data on the native RNA [19] is able to establish a simple model for the Mg^{2+} dependent structural transition from an extended form of the molecule to a more compact form. In the absence of Mg^{2+}, MS2 RNA appears to be a rodlike, perhaps cylindrical particle of about 300 nm length. The radius of the cross-section may be estimated from R_{cl} to be about $r = 4.4$ to 5.4 nm. The smaller radius is calculated according to the relation $r = R_{cl}/\sqrt{2}$, corresponding to a homogeneous cross-section; the larger value results from the relation $r = R_{cl}/\sqrt{3}$, which holds for an inhomogeneous cross-section resembling a spoke-wheel. Though certainly both assumptions are oversimplifications, the latter assumption might be more realistic. It would be in fair accord with the extended form of an RNA model in which double helical segments (hairpin loops) are linked together by single stranded segments (caterpillar model, *cf.* [3, 38]). On this assumption, the loops might have a mean length of about 5.4 nm.

In the presence of Mg^{2+} the RNA adopts a more compact configuration. According to our present results, Mg^{2+} causes a decrease of the length of the RNA particle and an increase of its cross-section. Native RNA at ionic strength 0.1 has previously been found to be an anisometric coil-like particle with a radius of gyration $R_G = 18.1$ nm, cross-section radius of gyration $R_{cl} = 8.43$ nm and thickness radius of gyration R_t of about 4 nm. The axes of the particle were estimated as about 63, 31 and 14 nm [19]. A comparison of these dimensions with those for the extended form of the RNA in the absence of Mg^{2+} shows a decrease of the longitudinal dimension of the particle to 1/5 of the initial length and an increase of the lateral dimension by a factor of 3. The thickness of the "native" RNA particle appears to be larger than the cross-section diameter of the extended form by a factor less than 1.5.

It should be noted that the model for the RNA in the absence of Mg^{2+} can be folded in several ways to particles of similar dimensions as found for the "native" RNA, particularly when the domains of hairpin loops are allowed to overlap. This would enable contacts and interactions even between formerly distant parts of the molecule. It can be

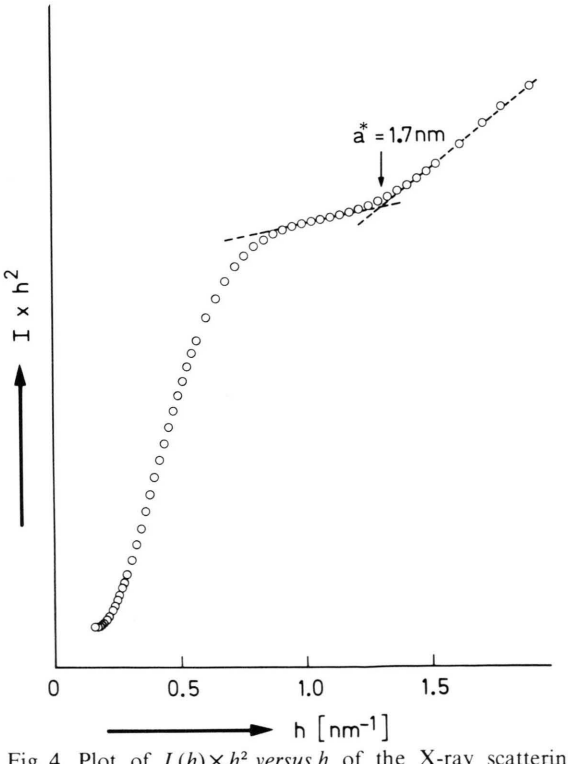

Fig. 4. Plot of $I(h) \times h^2$ *versus* h of the X-ray scattering curve of MS2 RNA in 2 mM phosphate buffer at 70 °C.

expected that such interactions result in the formation of additional base pairs. A Mg^{2+} induced increase of base-pairing in MS2 RNA, particularly at Mg^{2+}/phosphate ratios below 0.25, has been established by UV absorption [35]. That high concentrations of Mg^{2+} ions also enhance the intermolecular interactions and favour the formation of aggregates is a phenomenon well-known from other RNAs [39–41].

The melting of RNA at higher temperatures is clearly reflected by the drastic changes of the scattering behaviour and structural parameters (*cf.* Fig. 3 and Table II). Particularly the decrease of the mass per unit length to values typical of single-stranded chains (*e.g.* $M_c = 910\ g\ mol^{-1}\ nm^{-1}$ for RNA denatured by formaldehyde, *cf.* [36]) reflects the melting process very convincingly.

In order to check whether the melting of RNA has led to the formation of random coils the scattering curves taken at elevated temperatures were plotted as $I(h) \times h^2$ *vs.* h. Only one curve, namely that for the RNA in phosphate buffer at 70 °C (*cf.* Fig. 4), showed in this Kratky plot the behaviour characteristic of coiled chain molecules (*cf.* [42]). The transition point (marked by an arrow in the figure) corresponds to a persistence length of about 1.7 nm. Certainly this value appears to be quite small. For instance, a persistence length of 5.9 nm has previously been found for formaldehyde-denatured RNA at 60 °C [36]. On the other hand, a transition from a more extended to a tightly coiled structure could well be responsible for the observed slight increase of the mass per unit length at the highest temperature (*cf.* Table II).

[1] A. Riggs, H. Suzuki, and M. Cohn, J. Mol. Biol. **53,** 401–417 (1970).
[2] M. Poliakow, M. Champagne, and M. Daune, Eur. J. Biochem. **26,** 212–219 (1972).
[3] R. A. Cox and W. Hirst, Biochem. J. **160,** 505–519 (1976).
[4] R. A. Cox, Prog. Biophys. Molec. Biol. **32,** 193–231 (1977).
[5] A. Muto and R. A. Zimmerman, J. Mol. Biol. **121,** 1–15 (1978).
[6] W. Fiers, in Physico-chemical Properties of Nucleic Acids (Duchesne, J., ed.) **Vol. 2,** 213–235, Academic Press, London 1973.
[7] D. C. Lynch and P. R. Schimmel, Biochemistry **13,** 1841–1852 (1974).
[8] R. Römer and R. Hach, Eur. J. Biochem. **55,** 271–284 (1975).
[9] A. Stein and D. M. Crothers, Biochemistry **15,** 157–159 and 160–167 (1976).
[10] S. R. Holbrook, J. L. Sussman, R. W. Warrant, G. M. Church, and S. H. Kim, Nucleic Acids Research **4,** 2811–2820 (1977).
[11] Th. Olson, M. J. Fournier, K. H. Langley, and N. C. Ford, J. Mol. Biol. **102,** 193–203 (1976).
[12] J. L. Leroy, M. Guéron, G. Thomas, and A. Favre, Eur. J. Biochem. **74,** 567–574 (1977).
[13] K. W. Rhee, R. O. Potts, Ch. Ch. Wang, M. J. Fournier, and N. C. Ford, Nucleic Acids Research **9,** 2411–2420 (1981).
[14] S. H. Allen and K. P. Wong, J. Biol. Chem. **253,** 8759–8766 (1978).
[15] M. F. Tam, J. A. Dodd, and W. E. Hill, J. Biol. Chem. **256,** 6430–6434 (1981).
[16] V. D. Vasiliev and O. M. Zalite, FEBS Lett. **121,** 101–104 (1980).
[17] Q. M. Yi and K. P. Wong, Biochem. Biophys. Res. Commun. **104,** 733–739 (1982).
[18] K. Donceel, P. Nieuwenhuysen, and J. Clauwaert, Biochem. J. **205,** 495–501 (1982).
[19] P. Zipper, W. Folkhard, and J. Clauwaert, FEBS Lett. **56,** 283–287 (1975).
[20] W. Folkhard, I. Pilz, O. Kratky, R. Garrett, and G. Stöffler, Eur. J. Biochem. **59,** 63–71 (1975).
[21] P. Zipper and H. Bünemann, Eur. J. Biochem. **51,** 3–17 (1975).
[22] P. Zipper, G. Ribitsch, J. Schurz, and H. Bünemann, Z. Naturforsch. **37 c,** 824–832 (1982).
[23] H. Slegers and W. Fiers, Biopolymers **9,** 1373–1389 (1970).
[24] O. Kratky, Z. Elektrochem. **62,** 66–73 (1958).
[25] O. Kratky and Z. Skala, Z. Elektrochem. **62,** 73–77 (1958).
[26] O. Kratky, I. Pilz, and P. J. Schmitz, J. Colloid Interface Sci. **21,** 24–34 (1966).
[27] P. Zipper, Acta Phys. Austriaca **30,** 143–151 (1969).
[28] P. Zipper, Acta Phys. **36,** 27–38 (1972).
[29] O. Glatter, J. Appl. Cryst. **7,** 147–153 (1974).
[30] P. Zipper and O. Glatter, Abstr. 4th Int. Conf. on Small-Angle Scattering of X-Rays and Neutrons, Gatlinburg 1977, p. 49, Abstract PF-1.
[31] O. Glatter and O. Kratky (eds.), Small Angle X-ray Scattering, Academic Press, London 1982.
[32] O. Kratky, H. Leopold, and H. Stabinger, Z. Angew. Phys. **27,** 273–277 (1969).
[33] H. Eisenberg and G. Cohen, J. Mol. Biol. **37,** 355–362 (1968).
[34] K. O. Pedersen, J. Phys. Chem. **62,** 1282–1290 (1958).
[35] R. De Clercq, Thesis Univ. Gent, 1976.
[36] P. Zipper, W. Folkhard, and J. Clauwaert, Hoppe-Seyler's Z. Physiol. Chem. **354,** 1262–1263 (1973).
[37] P. Zipper, W. Folkhard, and J. Clauwaert, J. Appl. Cryst. **7,** 168 (1974).
[38] J. Witz and C. Strazielle, in Subunits in Biological Systems (Fasman, G. D. and Timasheff, S. N., eds.) Part B, pp. 205–252, Marcel Dekker Inc., New York 1973.
[39] R. Österberg, B. Sjöberg, and R. A. Garrett, Eur. J. Biochem. **68,** 481–487 (1976).
[40] P. Laggner, L. Nilsson, and R. Rigler, 5th Int. Conf. on Small-Angle Scattering, Berlin 1980, Abstract P III-13.
[41] P. Wilhelm, I. Pilz, G. Degovics, and F. van der Haar, Z. Naturforsch. **37 c,** 1293–1296 (1982).
[42] O. Kratky, Pure Appl. Chem. **12,** 483–523 (1966).